HHS Public Access

Author manuscript

J Surg Res. Author manuscript; available in PMC 2025 January 01.

Published in final edited form as:

J Surg Res. 2024 January ; 293: 618–624. doi:10.1016/j.jss.2023.09.001.

Expression of the calcium-sensing receptor on normal and abnormal parathyroid and thyroid tissue

A. L. Worth, MD[a,*], **M. Ayrapetyan, MD**[b,*], **S. J. Maygarden, MD**[b], **Z. Li, PhD**[c], **Z. Wu, PhD**[c], **C. B. Agala, PhD**[d], **L. T. Kim, MD**[e]

[a]University of North Carolina at Chapel Hill, School of Medicine, 321 S Columbia St, Chapel Hill, NC 27599, USA

[b]University of North Carolina at Chapel Hill, Department of Pathology and Laboratory Medicine, 160 Medical Dr, Chapel Hill, NC 27599, USA

[c]University of North Carolina at Chapel Hill, Biomedical Research Imaging Center, Department of Radiology, 125 Mason Farm Road, Marsico, Hall, Suite 1200, Chapel Hill, NC, USA

[d]University of North Carolina at Chapel Hill, Division of Epidemiology and Biostatistics, 170 Manning Dr. Chapel Hill, NC 27599-7213, USA

[e]University of North Carolina at Chapel Hill, Division of Surgical Oncology and Endocrine Surgery, Department of Surgery, 170 Manning Dr. CB#7213 Chapel Hill, NC 27599-7213, USA

Abstract

Background—Current imaging techniques have several limitations in detecting parathyroid glands. We have investigated the calcium-sensing receptor (CaSR) as a potential target for specifically labeling parathyroid glands for radiologic detection. For accurate imaging it is vital that a large differential expression exists between the target tissue and adjacent structures. We sought to investigate the relative abundance of the CaSR in normal and abnormal parathyroid tissue, as well as normal and abnormal thyroid.

Materials and Methods—Existing clinical specimens were selected that represented a wide variety of pathologically and clinically confirmed malignant and benign thyroid and parathyroid specimens. Sections were stained for the CaSR using immunohistochemistry and scored for

Corresponding author: Anne Worth | 919-966-5221 | anne_worth@med.unc.edu | 170 Manning Dr., CB #7213, Chapel Hill, NC 27599-7213.

*These authors contributed equally to this work

Author contributions: Anne Worth scored stained slides and drafted the text of the manuscript. Dr. Ayrapetyan and Dr. Maygarden obtained the archived tissue samples and coordinated staining and scoring of the slides. Dr. Li and Dr. Wu spearheaded development of the novel PET agent which binds to CaSR. Dr. Agala helped with biostatistical analysis of the final data. Dr. Kim generated the initial idea for the study, advised on and oversaw all the above processes, and provided integral contributions to the original abstract and the text of this manuscript.

Disclosures: None

Meeting Presentation: These data were presented as an oral presentation at the 2023 Academic Surgical Congress.

intensity and abundance of expression. (H score = intensity scored from 0 to 3 multiplied by the % of cells at each intensity. Range 0–300).

Results—All parathyroid specimens expressed the CaSR to a high degree. Normal parathyroid had the highest H score (270, s.d. 25.4). Abnormal parathyroid specimens were slightly lower but still much higher than normal thyroid (H score 38.3, s.d. 23.3). Medullary thyroid cancer also expressed the CaSR significantly higher than normal thyroid (H score 182, s.d. 69.1, $p<0.001$) but below parathyroid levels. Hürthle cell carcinoma expressed the CaSR to a lesser degree but higher than normal thyroid (H score 101, s.d. 46.4p=0.0037).

Conclusions—The CaSR is differentially expressed on parathyroid tissue making it a feasible target for parathyroid imaging. False positives might be anticipated with medullary and Hürthle cell cancers.

Keywords

Calcium-sensing receptor; parathyroid; thyroid; hyperparathyroidism; PET imaging

Introduction

Primary hyperparathyroidism is a disease characterized by overproduction of parathyroid hormone (PTH) by one or more parathyroid glands. It is the primary cause of hypercalcemia in adults. The disease is highly prevalent with conservative estimates suggesting 233 per 100,000 women and 85 per 100,000 men suffer from the condition.[1] While patients are often asymptomatic, hyperparathyroidism has been associated with a significant increase in risk for hip and other bone fractures as well as increased risk of cardiovascular events.[2] Other symptoms include fatigue, constipation, weakness, depression, and inability to concentrate.

Surgical resection of abnormal glands via bilateral neck exploration with visualization of all four parathyroid glands is the historic gold standard for treatment of the condition. Since the 1990's, minimally invasive parathyroidectomy (also known as focused or directed parathyroidectomy) has been more commonly performed and has been shown to have similar curative outcomes.[3] Among specialist surgeons, focused parathyroidectomy has become the most common approach.[4]

In the evaluation of patients with primary hyperparathyroidism, imaging is critical for patients undergoing directed parathyroidectomy. With a four-gland operation, preoperative imaging has classically been thought of us unnecessary as stated in 1986 by John Doppman, an interventional radiologist: "In my opinion, the only localizing study indicated in a patient with untreated primary hyperparathyroidism is to localize an experienced parathyroid surgeon."[5] Nevertheless, preoperative imaging has become routine in many centers regardless of the operative approach.[6] In addition, ultrasound can be useful to rule out concomitant thyroid disease and the authors would advocate its use in all cases.

Current imaging techniques include ultrasound, contrast-enhanced CT (4-D CT), and [99]technetium-sestamibi nuclear medicine scanning, ideally with SPECT-CT. None are able to detect normal parathyroid glands and all have limitations in detecting abnormal

parathyroid glands, particularly with multigland disease. For a detailed review of imaging techniques see Zander et al 2021.[7]

One possible approach to more sensitive detection is the use of a radiographically detectable, tissue-specific marker. Sestamibi accumulates in parathyroid adenomas but is not specific to parathyroid. Specific tracers that bind to parathyroid glands preferentially are not in clinical use. Some studies have explored the possibility of exploiting the CaSR as an imaging target. One study examined the ability to radiolabel the CaSR in vitro using a small molecule.[8] In another study, the calcimimetic cinacalcet which binds the CaSR was labeled for PET imaging. This showed uptake in the parathyroid/thyroid region, but specific parathyroid binding was not demonstrated.[9] Targeting the CaSR in humans has not yet been demonstrated. Positron emission tomography (PET) is a powerful and rapidly developing technology that can be used for quantitative *in vivo* measurement of site-specific biochemical markers. This can be used to detect specific metabolic pathways (e.g. fluorodeoxyglucose) or cell surface receptors (e.g. dotatate).[10]

We aim to develop a novel PET agent that is highly sensitive and specific to parathyroid. One obvious target for a parathyroid specific tracer is the CaSR. This is a transmembrane G-protein coupled receptor that responds to the calcium concentration in the serum. The CaSR is expressed primarily in the parathyroid and kidney, although a wide variety of tissues express this receptor including thyroid C-cells.[11] The high concentration of the CaSR on parathyroid cells suggests it is a promising target for an imaging agent. For the CaSR to be a good imaging target, there must be a significant difference in receptor concentration between the target (parathyroid glands) and surrounding structures (thyroid and others). The differential expression between parathyroid and thyroid is not known. Our hypothesis is that the CaSR is expressed to a significantly higher degree on parathyroid tissue than thyroid tissues.

Materials and Methods

Existing archival clinical specimens were selected based on availability. Parathyroid-derived specimens included normal parathyroid (n=9), parathyroid adenoma (n=9), primary parathyroid hyperplasia (n=10), secondary parathyroid hyperplasia (n=9), and parathyroid carcinoma (n=5). The distinction between parathyroid adenoma, primary parathyroid hyperplasia and secondary parathyroid hyperplasia were based primarily on clinical parameters. For example, an adenoma was defined as a single hypercellular parathyroid, removed in the setting of primary hyperparathyroidism, with a resultant biochemical cure. In addition, the following thyroid tumors were selected: normal thyroid (n=9), papillary carcinoma (n=9), follicular adenoma (n=8), follicular carcinoma (n=9), multinodular goiter (n=8), Hürthle cell adenoma (n=8), Hürthle cell carcinoma (n=8), medullary thyroid cancer (MTC) (n=9), and poorly differentiated or anaplastic cancer (n=8). Lung (n=5), submandibular gland (n=5), and parotid gland (n=5) tissues were also tested. The latter three were chosen because of findings from animal models that suggested the presence of the CaSR in these tissues (Unpublished results, data not shown). Specimens from patients under 18 years of age or those needed for ongoing clinical use were excluded from the study.

Chromogenic Immunohistochemistry (IHC) was performed on paraffin-embedded tissues that were sectioned at 5 microns. This IHC was carried out using the Leica Bond Rx Autostainer system. Slides were dewaxed in Bond Dewax solution (AR9222) and hydrated in Bond Wash solution (AR9590). Heat induced antigen retrieval was performed at 100°C in Bond-Epitope Retrieval solution 1 pH-6.0 (AR9961). After pretreatment, slides were incubated with Anti-CaSR antibody (ab19347, Abcam) at 1:3000 for 15m followed with ready-to use secondary antibodies Novolink Post Primary and Novolink Polymer (RE7260-CE, Leica). Antibody detection with 3,3'-diaminobenzidine (DAB) was performed using the Bond Intense R detection system (DS9263). Stained slides were dehydrated and coverslipped with Cytoseal 60 (23–244256, Thermo Fisher Scientific). A positive control tissue was included for this run. H&E stains were performed using the Leica Autostainer XL. The slides were stained with Hematoxylin (7211, Richard-Allen Scientific) for 2 mins and Eosin -Y (7111, Richard-Allen Scientific) for 1 min. Clarifier 2 (7402) and Bluing (7111) solutions from Richard-Allen Scientific were used to differentiate the reaction. After staining, slides were then dehydrated and coverslipped with Cytoseal 60 (23–244256, Thermo Fisher Scientific).

The stained slides were then scored for CaSR expression and assigned an "H" score ranging between 0 and 300.[12] This score was calculated by observing the intensity of staining (0–3) and visually estimating the proportion of cells in each specimen that were stained at each intensity. For example, if 30% of the cells stain 1+, 20% stain 2+ and 40% stain 3+ the H score would be 30+40+120=190. All tissues were evaluated at scanning magnification (20x) to estimate percentage of area that is stained and also at higher magnifications (200–400x) to confirm staining intensity, quality, and lack of any false/artefactual staining. Only membranous staining was considered positive.

The mean, median, and standard deviation in H-score was then calculated for each category of specimens. The Shapiro-Wilk test was used to test for normal distribution of scores for each tissue type (table 1). $p>0.05$ with this test suggests the data are normally or approximately normally distributed, otherwise they are non-normally distributed. Statistical significance of differences in H scores between tissue types was calculated using the Mann Whitney U test for pairwise tests if the Shapiro-Wilk test showed non-normal distribution for H-Scores from one or both tissue types. The independent T-test was used if values of H-Scores from both tissue types were normally distributed. Each comparison is shown in table 2.

The study was reviewed and approved by the Institutional Review Board of the University of North Carolina with waiver of informed consent.

Results

The average H-score for specimens derived from parathyroid tissue was significantly higher than that for normal thyroid (Table 1 and 2, Figures 1 and 2). Normal parathyroid had the highest H score (271, S.D. 25.4). The H-score for normal thyroid was among the lowest measured (38.3, S.D. 23.3.) Staining of abnormal parathyroid specimens was slightly lower than that for normal parathyroid. Parathyroid adenomas (H score 239, S.D. 26.7)

and primary parathyroid hyperplasia (H score 237, S.D. 23.7) and secondary parathyroid hyperplasia (H score 246, S.D. 25.4) had 88%, 87% and 91% (respectively) of the H score of normal parathyroid and these differences were statistically significant. Interestingly, parathyroid carcinoma (H score 238 ± 57.728) maintained a high expression of the CaSR. Overall, the differences between normal and abnormal parathyroid were small though statistically significant. Not surprisingly given its cell of origin, MTC averaged the highest H-score of the non-parathyroid tissues (H score 182, S.D. 69.1) and was statistically different than both normal parathyroid and thyroid. Hürthle cell cancer (H score 101 ± 46.398) expressed the CaSR to a lesser degree but also higher than normal thyroid. Expression of the CaSR in lung, submandibular, and parotid glands was low (see table 1 and figure 2).

Discussion

Our data show a differential expression of the CaSR in both normal and abnormal parathyroid tissue versus normal and pathological thyroid derived tissues. MTC also expressed the CaSR to a significant degree though still lower than parathyroid. MTC originates from the parafollicular C cells of the thyroid which have been shown to express CaSR so this is unsurprising.[13] The expression of the CaSR in Hürthle cell cancer was not expected, though the concentration is still relatively low compared to parathyroid. Based on our data, MTC and Hürthle cell cancer might give false positive imaging results. However, the clinical context is likely to mitigate any confusion except in specific clinical situations (e.g. MEN IIa).

Animal studies showed accumulation of labeled cinacalcet (which binds to the CaSR) in salivary glands and lung (Pees at al, and our unpublished data).[9] This raised the possibility of CaSR expression in these tissues. In tissues from mice, we did detect substantial CaSR expression in lung as shown by IHC (unpublished data, not shown). We did not demonstrate expression of the CaSR in these tissues in humans. This suggests that tissue expression of the CaSR differs among species.

The observed difference in CaSR expression between normal and abnormal parathyroid is small. At this time, it is not known whether this difference in expression will result in a clinically significant difference in PET signal. The slightly lower expression of the CaSR on abnormal parathyroids may be offset by the increased cellularity of abnormal parathyroids. We would expect that a PET/CT using a CaSR-targeted agent might have difficulty in differentiating a very small adenoma from a normal parathyroid. But clinical studies will need to be undertaken to see what the true strengths and weaknesses of a CaSR-targeted PET agent will be.

If an agent such as this is successful, we would not expect it to replace all other parathyroid imaging modalities. In particular, ultrasound will likely remain the primary imaging technique because of its ability to detect concurrent thyroid pathology, as well as its high spatial resolution, low cost, and wide availability. But a PET-detectable agent that could detect essentially all parathyroid tissue could be very valuable in certain circumstances. For example, the ability to detect small ectopic glands could be much improved from current

technology. Parathyromatosis could be diagnosed preoperatively. And a hand-held probe could be used intraoperatively in selected cases (such as a reoperative procedure) or as an aid to locating and identifying normal parathyroids during difficult thyroidectomies.

A strength of this study is the systematic examination of a wide variety of tissue types. One weakness is the small sample size in some categories. However, the differences seen between thyroid and parathyroid as a whole are robust and conclusions are not likely to significantly change with higher sample numbers.

Conclusions

Parathyroid expression of the CaSR is high. Expression of the CaSR by parathyroid adenoma and primary parathyroid hyperplasia is slightly lower than normal parathyroid, but still higher than thyroid-derived tissues. Expression of the CaSR in MTC is substantial and much higher than thyroid follicular-derived tumors, though still lower than parathyroid. Hürthle cell cancer expressed the CaSR to a lesser degree but also higher than normal thyroid. Given the high intensity of CaSR expression in normal and abnormal parathyroids relative to thyroid-derived tissue, the CaSR represents a promising target for parathyroid imaging.

Acknowledgements:

We thank Lauren Ralph and Yongjuan Xia in the Pathology Services Core (PSC) for expert technical assistance with Histopathology/Digital Pathology including tissue sectioning, immunohistochemical staining, and imaging.

Funding:

This study was funded in part by the National Institute of Diabetes and Digestive and Kidney Diseases 1R01DK128447-01A1. The PSC is supported in part by an NCI Center Core Support Grant (P30CA016086)

References

1. Yeh MW, Ituarte PHG, Zhou HC, et al. Incidence and prevalence of primary hyperparathyroidism in a racially mixed population. J Clin Endocrinol Metab. 2013;98(3):1122–1129. doi:10.1210/jc.2012-4022 [PubMed: 23418315]
2. Axelsson KF, Wallander M, Johansson H, et al. Analysis of comorbidities, clinical outcomes, and parathyroidectomy in adults with primary hyperparathyroidism. JAMA Netw Open. 2022;5(6):e2215396. doi:10.1001/jamanetworkopen.2022.15396 [PubMed: 35657624]
3. Park H-S, Hong N, Jeong JJ, Yun M, Rhee Y. Update on preoperative parathyroid localization in primary hyperparathyroidism. Endocrinol Metab (Seoul). 2022;37(5):744–755. doi:10.3803/EnM.2022.1589 [PubMed: 36327985]
4. Greene AB, Butler RS, McIntyre S, et al. National trends in parathyroid surgery from 1998 to 2008: a decade of change. J Am Coll Surg. 2009;209(3):332–343. doi:10.1016/j.jamcollsurg.2009.05.029 [PubMed: 19717037]
5. Doppman JL. Reoperative parathyroid surgery; localization procedures. In: Rothmund M, Wells SA Jr., eds. Parathyroid Surgery. Vol 18. Progress in Surgery. S. Karger AG; 1986:117–132. doi:10.1159/000412364
6. Ishii H, Stechman MJ, Watkinson JC, Aspinall S, Kim DS. A Review of Parathyroid Surgery for Primary Hyperparathyroidism from the United Kingdom Registry of Endocrine and Thyroid Surgery (UKRETS). World J Surg. 2021;45(3):782–789. doi:10.1007/s00268-020-05885-5 [PubMed: 33263777]

7. Expert Panel on Neurological Imaging, Zander D, Bunch PM, et al. ACR appropriateness criteria® parathyroid adenoma. J Am Coll Radiol 2021;18(11S):S406–S422. doi:10.1016/j.jacr.2021.08.013 [PubMed: 34794597]

8. Yusof AM, Kothandaraman S, Zhang X, et al. Development of a calcium-sensing receptor molecular imaging agent. Surgery. 2013;154(6):1378–1384; discussion 1384. doi:10.1016/j.surg.2013.06.044 [PubMed: 24238055]

9. Pees A, Beaino W, Kooijman EJM, et al. Synthesis and evaluation of [18F]cinacalcet for the imaging of parathyroid hyperplasia. Nucl Med Biol. 2021;102–103:97–105. doi:10.1016/j.nucmedbio.2021.10.003

10. Fortunati E, Argalia G, Zanoni L, Fanti S, Ambrosini V. New PET radiotracers for the imaging of neuroendocrine neoplasms. Curr Treat Options Oncol. 2022;23(5):703–720. doi:10.1007/s11864-022-00967-z [PubMed: 35325412]

11. Brown EM, MacLeod RJ. Extracellular calcium sensing and extracellular calcium signaling. Physiol Rev. 2001;81(1):239–297. doi:10.1152/physrev.2001.81.1.239 [PubMed: 11152759]

12. Sangoi AR, Shrestha B, Yang G, Mego O, Beck AH. The novel marker GATA3 is significantly more sensitive than traditional markers mammaglobin and GCDFP15 for identifying breast cancer in surgical and cytology specimens of metastatic and matched primary tumors. Appl Immunohistochem Mol Morphol. 2016;24(4):229–237. doi:10.1097/PAI.0000000000000186 [PubMed: 25906123]

13. Mun H-C, Leach KM, Conigrave AD. L-Amino Acids Promote Calcitonin Release via a Calcium-Sensing Receptor: Gq/11-Mediated Pathway in Human C-Cells. Endocrinology. 2019;160(7):1590–1599. doi:10.1210/en.2018-00860 [PubMed: 31127815]

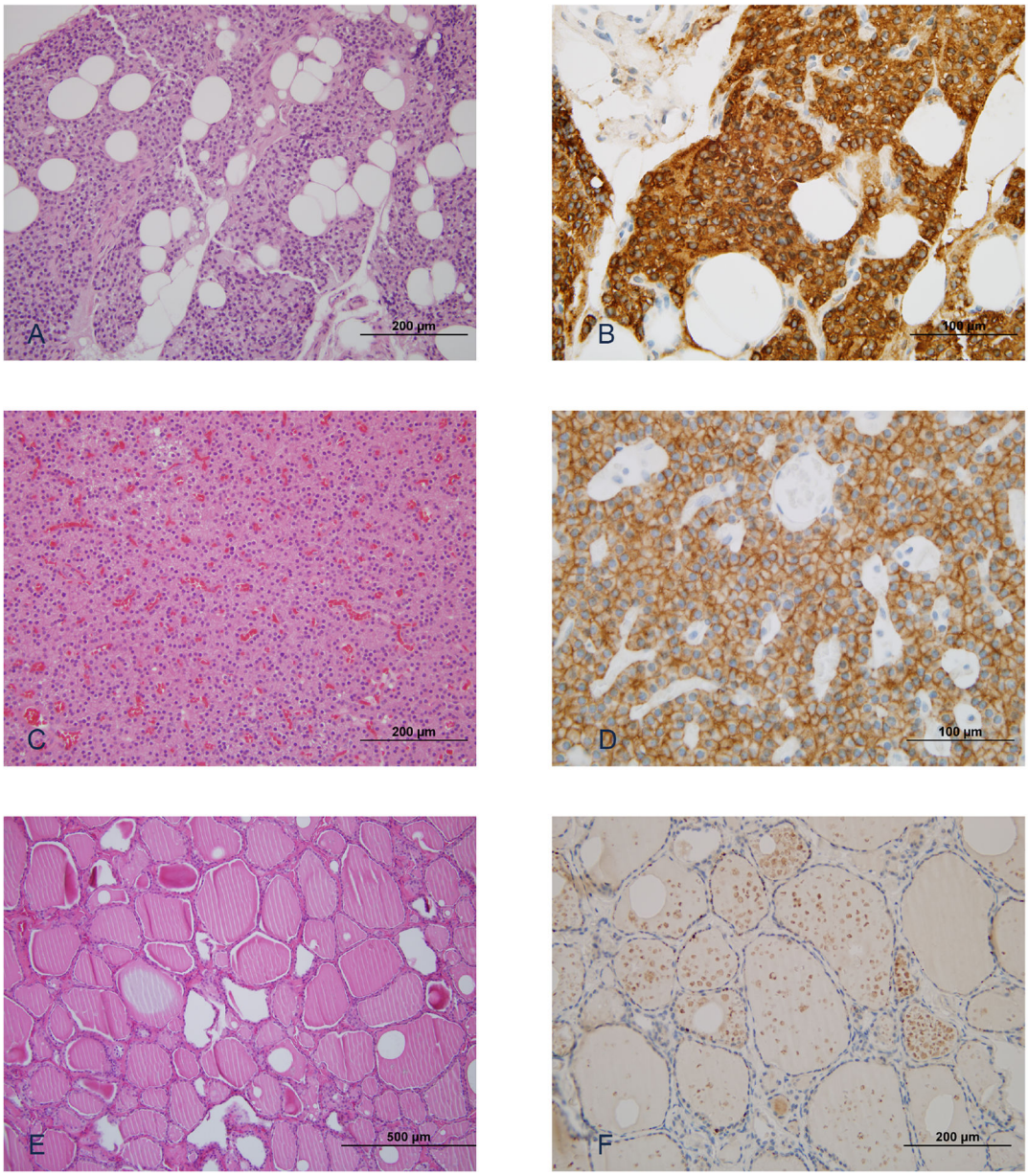

Figure 1.

H&E staining (left) and immunohistochemistry staining (right) for the calcium-sensing receptor. A,B: normal parathyroid. C,D: parathyroid adenoma. E,F: normal thyroid

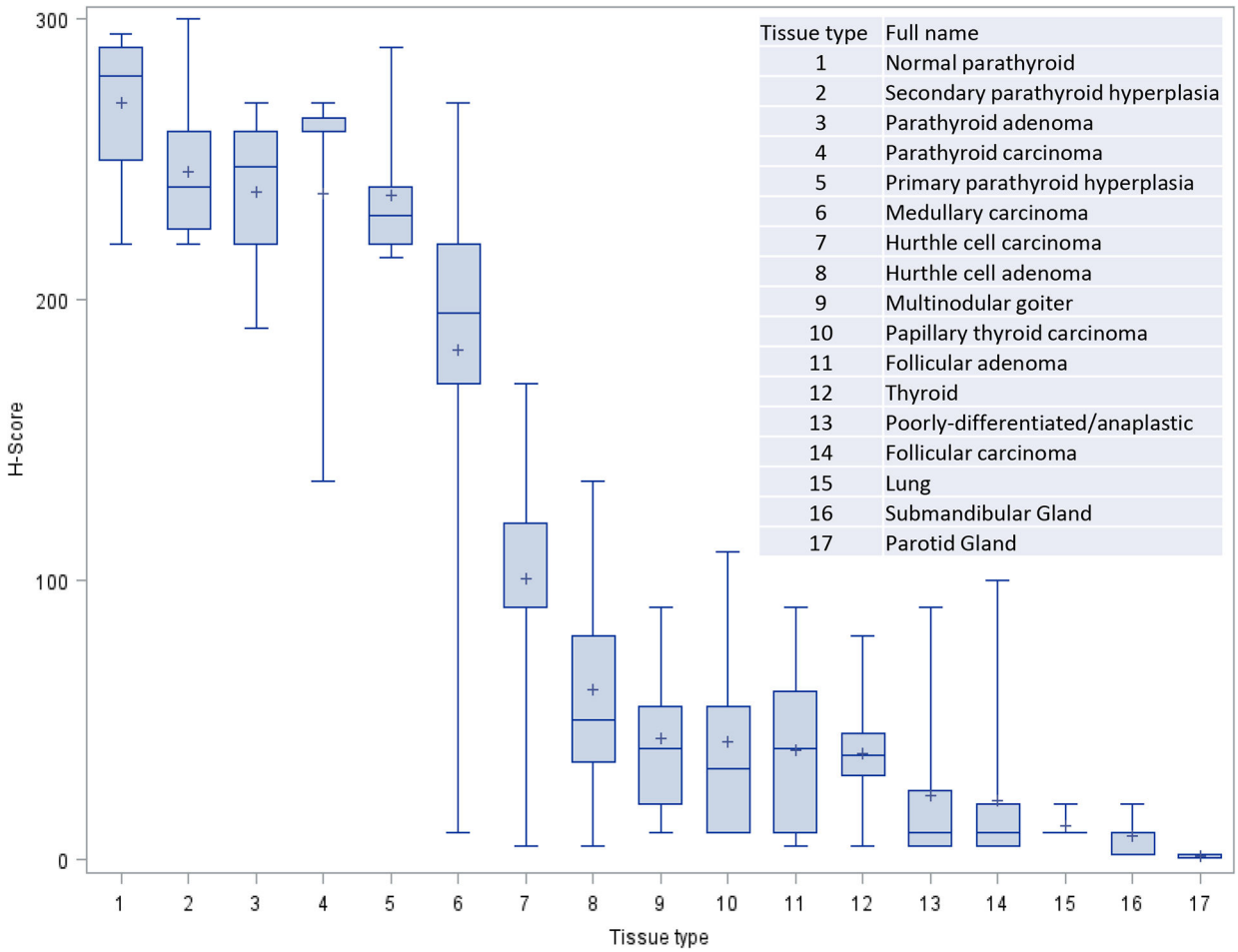

Figure 2.

Box plot for H score by tissue type. Rectangles indicate the 25th to 75th percentile. Ranges are shown by vertical lines. Median values are indicated by horizontal lines and means by "+".

Table 1.

Summary and normality test statistics for H-Score by entity type.

#	Tissue	N Obs	Mean	Std Dev	Median	25th Pctl	75th Pctl	Range	Min.	Max.	Shapiro-Wilk test p-value	Interpretation
1	Normal parathyroid	10	270.5	25.4	280	250	290	75	220	295	0.0644	normal or approximately normal
2	Secondary parathyroid hyperplasia	10	245.5	25.4	240	225	260	80	220	300	0.2076	normal or approximately normal
3	Parathyroid adenoma	10	238.5	26.7	247.5	220	260	80	190	270	0.1859	normal or approximately normal
4	Parathyroid carcinoma	5	238.0	57.7	260	260	265	135	135	270	**0.0012**	non-normal
5	Primary parathyroid hyperplasia	10	237.0	23.7	230	220	240	75	215	290	**0.0284**	non-normal
6	Medullary carcinoma	10	182.0	69.1	195	170	220	260	10	270	**0.0354**	non-normal
7	Hurthle cell carcinoma	9	100.6	46.4	90	90	120	165	5	170	0.1787	normal or approximately normal
8	Hurthle cell adenoma	9	61.1	40.0	50	35	80	130	5	135	0.7824	normal or approximately normal
9	Multinodular goiter	9	43.3	25.6	40	20	55	80	10	90	0.7185	normal or approximately normal
10	Papillary thyroid carcinoma	10	42.5	36.5	32.5	10	55	100	10	110	**0.0411**	non-normal
11	Follicular adenoma	9	39.4	31.5	40	10	60	85	5	90	0.2656	normal or approximately normal
12	Thyroid	10	38.3	23.3	37.5	30	45	75	5	80	0.5517	normal or approximately normal
13	Poorly-differentiated/anaplastic	9	23.3	27.6	10	5	25	85	5	90	**0.0025**	non-normal
14	Follicular carcinoma	10	21.5	28.8	10	5	20	95	5	100	**<0.0001**	non-normal
15	Lung	5	12.0	4.5	10	10	10	10	10	20	**0.0001**	non-normal
16	Submandibular Gland	5	8.8	7.4	10	2	10	18	2	20	0.2844	normal or approximately normal
17	Parotid Gland	5	1.6	0.5	2	1	2	1	1	2	**0.0065**	non-normal

Table 2.

Comparison of H-Scores by tissue type.

	Tissue	Comparison	p-value	Statistical test	Comparison	p-value	Statistical test	Comparison	p-value	Statistical test
1	Normal parathyroid				vs normal thyroid	<0.0001	T-test			
2	Secondary parathyroid hyperplasia	vs normal parathyroid	**0.0413**	T-test						
3	Parathyroid adenoma	vs normal parathyroid	**0.0133**	T-test						
4	Parathyroid carcinoma	vs normal parathyroid	0.1391	Mann Whitney U test						
5	Primary parathyroid hyperplasia	vs normal parathyroid	**0.0131**	Mann Whitney U test						
6	Medullary carcinoma	vs normal parathyroid	**0.0007**	Mann Whitney U test	vs normal thyroid	0.0017	Mann Whitney U test			
7	Hurthle cell carcinoma	vs normal parathyroid	**<.0001**	T-test	vs normal thyroid	0.0037	T-test	vs Hurthle cell adenom	0.0717	T-test
8	Hurthle cell adenoma	vs normal parathyroid	**<.0001**	T-test	vs normal thyroid	0.1587	T-test			
9	Multinodular goiter	vs normal parathyroid	**<.0001**	T-test	vs normal thyroid	0.6611	T-test			
10	Papillary thyroid carcinoma	vs normal parathyroid	**0.0002**	Mann Whitney U test	vs normal thyroid	1	Mann Whitney U test			
14	Follicular carcinoma	vs normal parathyroid	0.0002	Mann Whitney U test	vs normal thyroid	0.0668	Mann Whitney U test	vs Follicular adenoma	0.1586	Mann Whitney U test
11	Follicular adenoma	vs normal parathyroid	**<.0001**	T-test	vs normal thyroid	0.93	T-test			
13	Poorly-differentiated/ anaplastic	vs normal parathyroid	**0.0003**	Mann Whitney U test	vs normal thyroid	0.1376	Mann Whitney U test			
12	Thyroid	vs normal parathyroid	**<.0001**	T-test						